*J. Fluid Mech.* (1987), *vol.* 180, *pp.* 451–469
*Printed in Great Britain*



# Resonant reflection of shallow-water waves due to corrugated boundaries

By SUNG B. YOON AND PHILIP L.-F. LIU

Joseph H. DeFrees Hydraulics Laboratory, School of Civil and Environmental Engineering, Cornell University, Ithaca, NY 14853, U.S.A.

(Received 29 July 1986 and in revised form 29 December 1986)

One-dimensional, nonlinear, shallow-water wave equations are derived from two-dimensional Boussinesq equations to investigate resonant reflections due to corrugated boundaries. Small, but short-wave undulations are introduced through water depth and channel width. Coupled nonlinear equations for the transmitted and reflected wave fields are derived and solved numerically. In the simple case where undulations are zero (the reflection is also zero), the governing equations are used to study the propagation of permanent shallow-water waves (cnoidal waves) and to examine the generation of higher harmonics in shallow-water waves. The present numerical results show that the nonlinear effects are very important in considering the resonant reflection of cnoidal waves from a rippled bed.

## 1. Introduction

The interaction between seabed topography and ocean waves is of considerable interest to coastal engineers. Certain topographies are capable of reflecting a significant amount of wave energy and, therefore, protecting the beach. Recently, the resonant reflection of water waves from periodic sandbars has been studied experimentally and theoretically by many researchers (e.g. Davies 1982; Davies & Heathershaw 1984; Mitra & Greenberg 1984; Mei 1985; Kirby 1986*a*, *b*; Vengayil 1986). Based on a linear wave theory, the reflected waves can be resonated by periodic sandbars if the wavelength of seabed undulations is one-half of that of the incident waves. Liu (1987) showed that resonant reflection also occurs in a long channel with an undulating width. Since water waves tend to become nonlinear in shallow coastal water, a nonlinear shallow-water theory describing the resonant interaction between waves and corrugated boundaries is wanting.

Lau & Barcilon (1972) studied the resonant reflection from a patch of periodic sandbars in shallow water. Coupled nonlinear equations were derived for the transmitted and the reflected waves. Since only the first two harmonics are included, their theory cannot be used to describe the reflection of cnoidal waves.

In this paper, we derive a set of coupled, nonlinear, shallow-water wave equations describing wave propagation in a long channel with corrugated boundaries. The boundary undulations are introduced through either a rippled topography or the short-wave variation in channel banks. Only the near-resonance case, where the incident wavenumber meets the Bragg condition either exactly or nearly, is studied. A numerical scheme is developed to integrate the simultaneous nonlinear differential equations; analytical solutions are obtained only for the linear problem. Two types of incident waves, a modulated wavetrain and a cnoidal wave, are studied.

In verifying the accuracy of the numerical scheme used in this paper, we examine

the harmonic-generation problems in a long shallow-wave channel with a constant depth. Our numerical solutions, including five harmonics, agree well with experimental data (Goda 1967). We also demonstrate that the present approach and computing scheme can accurately simulate a cnoidal wave propagating in a constant water depth.

In studying the resonant reflection of a modulated wavetrain from a rippled bed, we demonstrate that Lau & Barcilon's (1972) numerical results do not satisfy the law of energy conservation. Our results, including either two or five harmonics, give larger reflection coefficients than those predicted by Lau & Barcilon. Numerical results for the resonant reflection of cnoidal waves are also presented. Five harmonics are used in computations.

In the following section, using the Boussinesq equations, we derive a set of two-dimensional wave equations for the Fourier components of the free-surface displacement. In §3, the wave equations are reduced to one-dimensional equations in a long channel; the effects of depth and width undulations are included. Analytical solutions are obtained for linear problems. Numerical solutions for the resonant reflection of a modulated wavetrain as well as a cnoidal wavetrain are presented in §4. The inclusion of energy dissipation terms in the governing equations is discussed in Appendix.

## 2. Derivation of shallow-wave evolution equation

The Boussinesq equations, which describe weakly nonlinear, dispersive shallow-water waves, are used in the present study. Using $\omega'$ as the characteristic frequency, $a_0'$ as the characteristic wave amplitude and $h_0'$ as the characteristic water depth, the dimensionless form of the Boussinesq equations can be expressed as (e.g. see Peregrine 1972)

$$\frac{\partial \zeta}{\partial t}+\nabla\cdot[(h+\epsilon\zeta)\,\boldsymbol{u}] = O(\epsilon^2, \epsilon\mu^2, \mu^4), \tag{2.1}$$

$$\frac{\partial \boldsymbol{u}}{\partial t}+\epsilon\boldsymbol{u}\cdot\nabla\boldsymbol{u}+\nabla\zeta = \mu^2\left\{\tfrac{1}{2}h\frac{\partial}{\partial t}\nabla[\nabla\cdot(h\boldsymbol{u})]-\tfrac{1}{6}h^2\frac{\partial}{\partial t}\nabla(\nabla\cdot\boldsymbol{u})\right\}+O(\epsilon^2, \epsilon\mu^2, \mu^4), \tag{2.2}$$

where

$$\epsilon = \frac{a_0'}{h_0'} \ll 1, \quad \mu^2 = \frac{\omega'^2 h_0'}{g} \ll 1. \tag{2.3a, b}$$

$\zeta$ is the free-surface displacement, and $\boldsymbol{u}$ represents the depth-averaged horizontal velocity vector. In (2.1) and (2.2) $\nabla$ denotes the two-dimensional gradient vector. The small parameters $\epsilon$ and $\mu^2$, representing the nonlinearity and dispersion respectively, are assumed to be of the same order of magnitude. However, solutions obtained from (2.1) and (2.2) are still valid for cases where these two parameters are not of the same order of magnitude (Peregrine 1972).

Consider the total depth, $z = -h(x, y)$, as the sum of a local mean depth $\bar{h}(x, y)$ and a undulation $\tilde{h}(x, y)$; i.e.

$$h(x, y) = \bar{h}(x, y)+\tilde{h}(x, y). \tag{2.4}$$

In the present study, we assume that the amplitude of the topographical undulations is small in comparison with the local mean depth and that the variation of the total depth within the characteristic wavelength is small, i.e.

$$\left.\begin{aligned} \bar{h} \sim O(1), \quad \tilde{h} \sim O(\mu^2), \\ |\nabla\bar{h}| \sim O(\mu^2), \quad |\nabla\tilde{h}| \sim O(\mu^2). \end{aligned}\right\} \tag{2.5}$$

By using the above assumptions, the momentum equation (2.2) can be reduced to

$$\frac{\partial \boldsymbol{u}}{\partial t}+\epsilon \boldsymbol{u}\cdot\nabla\boldsymbol{u}+\nabla\zeta=\tfrac{1}{3}\mu^2\bar{h}^2\,\nabla\left(\nabla\cdot\frac{\partial \boldsymbol{u}}{\partial t}\right)+O(\epsilon^2,\epsilon\mu^2,\mu^4). \tag{2.6}$$

Assuming periodic motion in time, the free-surface displacement and the velocity vector can be expressed as Fourier series:

$$\zeta(x,y,t)=\tfrac{1}{2}\sum_n \zeta_n(x,y)\,\mathrm{e}^{-\mathrm{i}nt};\quad n=0,\pm1,\pm2,\ldots, \tag{2.7a}$$

$$\boldsymbol{u}(x,y,t)=\tfrac{1}{2}\sum_n \boldsymbol{U}_n(x,y)\,\mathrm{e}^{-\mathrm{i}nt};\quad n=0,\pm1,\pm2,\ldots, \tag{2.7b}$$

where $(\zeta_{-n}, \boldsymbol{U}_{-n})$ are the complex conjugates of $(\zeta_n, \boldsymbol{U}_n)$. Substituting (2.7) into (2.1) and (2.6), and collecting the different Fourier components, we have

$$-\mathrm{i}n\zeta_n+\nabla\cdot(h\boldsymbol{U}_n)+\tfrac{1}{2}\epsilon\sum_s \nabla\cdot(\zeta_s\,\boldsymbol{U}_{n-s})=O(\epsilon^2,\epsilon\mu^2,\mu^4), \tag{2.8}$$

$$-\mathrm{i}n\boldsymbol{U}_n+\tfrac{1}{2}\epsilon\sum_s \boldsymbol{U}_s\cdot\nabla\boldsymbol{U}_{n-s}+\nabla\zeta_n=-\mathrm{i}n\tfrac{1}{3}\mu^2\bar{h}^2\nabla(\nabla\cdot\boldsymbol{U}_n)+O(\epsilon^2,\epsilon\mu^2,\mu^4), \tag{2.9}$$

where $s=0,\pm1,\pm2,\ldots$. From (2.8) and (2.9), we find the following simple relationships:

$$\nabla\cdot\boldsymbol{U}_n=\frac{\mathrm{i}n\zeta_n}{\bar{h}}+O(\epsilon), \tag{2.10}$$

$$\boldsymbol{U}_n=-\frac{\mathrm{i}}{n}\nabla\zeta_n+O(\epsilon), \tag{2.11}$$

for $n\neq0$, and

$$\boldsymbol{U}_0=-\frac{\epsilon}{2\bar{h}}\sum_s \zeta_s\,\boldsymbol{U}_{-s}+O(\epsilon^2), \tag{2.12}$$

$$\zeta_0=-\tfrac{1}{4}\epsilon\sum_s \boldsymbol{U}_s\cdot\boldsymbol{U}_{-s}+O(\epsilon^2). \tag{2.13}$$

Combining (2.8) and (2.9) and using (2.4), (2.10) and (2.11), we obtain

$$(\bar{h}+\hat{h}-\tfrac{1}{3}\mu^2n^2\bar{h}^2)\nabla^2\zeta_n+\nabla(\bar{h}+\hat{h})\cdot\nabla\zeta_n+n^2\zeta_n-\epsilon\sum_{\substack{s=0\\ s\neq n}}\left\{\frac{n^2-s^2}{2\bar{h}}\zeta_s\,\zeta_{n-s}-\frac{n+s}{2(n-s)}\frac{\partial\zeta_s}{\partial x}\frac{\partial\zeta_{n-s}}{\partial x}\right\}$$
$$=O\left(\epsilon^2,\epsilon\mu^2,\mu^4,\epsilon\left|\frac{\partial\zeta}{\partial y}\right|^2\right). \tag{2.14}$$

The zeroth components $(\boldsymbol{U}_0,\zeta_0)$ have been excluded from the nonlinear terms in the above equation, since the zeroth components are $O(\epsilon)$. From (2.14), the leading-order equation gives

$$\nabla^2\zeta_n=-\frac{n^2}{\bar{h}}\zeta_n+O(\epsilon). \tag{2.15}$$

Substituting (2.15) into (2.14) and assuming that the primary wave propagation direction is $\pm x$, we have

$$\bar{h}\nabla^2\zeta_n+\nabla(\bar{h}+\hat{h})\cdot\nabla\zeta_n+n^2\left(1-\frac{\hat{h}}{\bar{h}}+\tfrac{1}{3}\mu^2n^2\bar{h}\right)\zeta_n$$
$$-\epsilon\sum_{\substack{s\neq n\\ s\neq0}}\left\{\frac{n^2-s^2}{2\bar{h}}\zeta_s\,\zeta_{n-s}-\frac{n+s}{2(n-s)}\frac{\partial\zeta_s}{\partial x}\frac{\partial\zeta_{n-s}}{\partial x}\right\}=O(\epsilon^2,\epsilon\mu^2,\mu^4), \tag{2.16}$$

where $$\frac{\partial \zeta_n}{\partial y} \sim O(\mu), \quad \frac{\partial^2 \zeta_n}{\partial y^2} \sim O(\mu^2), \tag{2.17a, b}$$

are assumed. Equation (2.16) is a set of nonlinear partial differential equations describing the combined refraction and diffraction of two-dimensional shallow-water waves. These partial differential equations are of the elliptical type and can be solved, in principle, with appropriate boundary conditions as a set of coupled boundary-value problems. For the case where the undulation is zero, $\tilde{h} = 0$ (2.16) can be reduced to the equation derived by Liu, Yoon & Kirby (1985). On the other hand if the depth is a constant, $\bar{h} = 1.0$ and $\tilde{h} = 0$, (2.16) is the same as that derived by Rogers & Mei (1978).

## 3. Near-resonant reflection in a long channel

### 3.1. *Governing equations*

If the mean depth $\bar{h}$ and the short-wave undulation $\tilde{h}$ vary only in the $x$-direction, (2.16) becomes

$$\bar{h}\nabla^2\zeta_n + \frac{\mathrm{d}(\bar{h}+\tilde{h})}{\mathrm{d}x}\frac{\partial \zeta_n}{\partial x} + n^2\left(1 - \frac{\tilde{h}}{\bar{h}} + \tfrac{1}{3}\mu^2 n^2 \bar{h}\right)\zeta_n - \epsilon \sum_{\substack{s\neq 0 \\ s\neq n}} \left\{\frac{n^2-s^2}{2\bar{h}}\zeta_s \zeta_{n-s} - \frac{n+s}{2(n-s)}\frac{\partial \zeta_s}{\partial x}\frac{\zeta_{n-s}}{\partial x}\right\} = O(\epsilon^2, \epsilon\mu^2, \mu^4). \tag{3.1}$$

For a long channel of width much less than the longitudinal lengthscale, (2.17$a$, $b$) remain valid. Let $b(x)$ be the width of the channel. If $y = b_1(x)$ and $b_2(x)$ describe the configuration of the channel banks, then $b(x) = b_2(x) - b_1(x)$. The no-flux boundary condition along the channel banks requires

$$U_n \frac{\mathrm{d}b_j}{\mathrm{d}x} - V_n = 0 \quad \text{along } y = b_j(x), \tag{3.2}$$

where $j = 1$ and 2, and $(U_n, V_n)$ are the components of the velocity vector $\boldsymbol{U}_n$. Assuming that $O(\mathrm{d}b_j/\mathrm{d}x)$ is small and using (2.11), the lateral boundary condition becomes

$$\frac{\partial \zeta_n}{\partial x}\frac{\partial b_j}{\partial x} - \frac{\partial \zeta_n}{\partial y} = O(\mu^4) \quad \text{along } y = b_j(x); \quad j = 1, 2. \tag{3.3}$$

Integrating (3.1) over the channel width, and applying Leibniz' rule and the lateral boundary condition (3.3), we have

$$\bar{h}\frac{\mathrm{d}^2\zeta_n}{\mathrm{d}x^2} + \left\{\frac{\mathrm{d}}{\mathrm{d}x}(\bar{h}+\tilde{h}) + \frac{\bar{h}}{\bar{b}}\frac{\mathrm{d}}{\mathrm{d}x}(\bar{b}+\tilde{b})\right\}\frac{\mathrm{d}\zeta_n}{\mathrm{d}x} + n^2\left(1 - \frac{\tilde{h}}{\bar{h}} + \tfrac{1}{3}\mu^2 n^2 \bar{h}\right)\zeta_n - \epsilon \sum_{\substack{s\neq 0 \\ s\neq n}} \left\{\frac{n^2-s^2}{2\bar{h}}\zeta_s \zeta_{n-s} - \frac{n+s}{2(n-s)}\frac{\mathrm{d}\zeta_s}{\mathrm{d}x}\frac{\mathrm{d}\zeta_{n-s}}{\mathrm{d}x}\right\} = O(\epsilon^2, \epsilon\mu^2, \mu^4), \tag{3.4}$$

where the total channel width $b(x)$ has been decomposed into two parts, a slowly varying local mean width $\bar{b}(x)$, and a fast undulating part $\tilde{b}(x)$ which satisfy the following assumptions:

$$b = \bar{b}(x) + \tilde{b}(x), \tag{3.5}$$

$$\left.\begin{aligned} \bar{b} \sim O(1), \quad \tilde{b} \sim O(\mu^2), \\ \frac{\mathrm{d}\bar{b}}{\mathrm{d}x} \sim O(\mu^2), \quad \frac{\mathrm{d}\tilde{b}}{\mathrm{d}x} \sim O(\mu^2). \end{aligned}\right\} \tag{3.6}$$

The total wave field can be separated into transmitted and reflected waves; i.e.

$$\zeta_n = \zeta_n^+ + \zeta_n^-. \tag{3.7}$$

Here the superscripts + and − denote the transmitted and the reflected waves respectively. The lowest-order terms in (3.4) provide the following simple relationship:

$$\frac{\mathrm{d}\zeta_n^\pm}{\mathrm{d}x} = \pm \frac{in}{\bar{h}^{\frac{1}{2}}} \zeta_n^\pm + O(\epsilon). \tag{3.8}$$

Substituting (3.8) into the nonlinear terms of (3.4), we have

$$\begin{aligned}
&\bar{h}\frac{\mathrm{d}^2}{\mathrm{d}x^2}(\zeta_n^+ + \zeta_n^-) + \left\{\frac{\mathrm{d}}{\mathrm{d}x}(\bar{h}+\tilde{h}) + \frac{\bar{h}}{\bar{b}}\frac{\mathrm{d}}{\mathrm{d}x}(\bar{b}+\tilde{b})\right\}\frac{\mathrm{d}}{\mathrm{d}x}(\zeta_n^+ + \zeta_n^-) \\
&+ n^2\left(1 - \frac{\tilde{h}}{\bar{h}} + \tfrac{1}{3}\mu^2 n^2 \bar{h}\right)(\zeta_n^+ + \zeta_n^-) - \frac{\epsilon}{2\bar{h}} \sum_{\substack{s\neq 0 \\ s\neq n}} \Big\{ n(n+s)\,(\zeta_s^+\,\zeta_{n-s}^+ + \zeta_s^-\,\zeta_{n-s}^-) \\
&- (n^2 + 4s^2 - 4ns)\,\zeta_s^-\,\zeta_{n-s}^+ \Big\} = O(\epsilon^2, \epsilon\mu^2, \mu^4).
\end{aligned} \tag{3.9}$$

The leading-order equation (3.8) suggests a solution of the following form:

$$\zeta_n^\pm = \Psi_n^\pm(x) \exp\left[\pm in \int \frac{1}{\bar{h}^{\frac{1}{2}}}\mathrm{d}x\right], \tag{3.10}$$

where $\Psi_n^\pm(x)$ are the complex wave amplitudes which are slowly varying functions such that

$$\frac{\mathrm{d}\Psi_n^\pm}{\mathrm{d}x} \sim O(\mu^2), \quad \frac{\mathrm{d}^2\Psi_n^\pm}{\mathrm{d}x^2} \sim O(\mu^4). \tag{3.11}$$

The boundary undulations $(\tilde{h}, \tilde{b})$ may be expressed as Fourier series:

$$\tilde{h} = \sum_{p\neq 0} \tfrac{1}{2}(H_p(x)) \exp\left[ip\Lambda_h \int \frac{1}{\bar{h}^{\frac{1}{2}}}\mathrm{d}x\right], \quad p = \pm 1, \pm 2, \ldots, \tag{3.12a}$$

$$\tilde{b} = \sum_{q\neq 0} \tfrac{1}{2}(B_q(x)) \exp\left[iq\Lambda_b \int \frac{1}{\bar{h}^{\frac{1}{2}}}\mathrm{d}x\right], \quad q = \pm 1, \pm 2, \ldots, \tag{3.12b}$$

where $H_p(x)$ and $B_q(x)$ are the amplitudes of the $p$th and the $q$th component in depth and width undulations respectively; $\Lambda_h$ and $\Lambda_b$ are the characteristic wavenumbers of the depth undulation and the width undulation respectively. $H_p(x)$ and $B_q(x)$ are the slowly varying functions and $\Lambda_h$ and $\Lambda_b$ are constants.

Substituting (3.10) and (3.12) into (3.9) and collecting $\exp[\pm in\int(1/\bar{h}^{\frac{1}{2}})\mathrm{d}x]$ components, we obtain a set of coupled evolution equations:

$$\begin{aligned}
&\bar{h}^{\frac{1}{2}}\frac{\mathrm{d}\Psi_n^+}{\mathrm{d}x} + \left\{\frac{1}{2}\left(\frac{\mathrm{d}\bar{h}^{\frac{1}{2}}}{\mathrm{d}x} + \frac{\bar{h}^{\frac{1}{2}}}{\bar{b}}\frac{\mathrm{d}\bar{b}}{\mathrm{d}x}\right) - \tfrac{1}{6}i\mu^2 n^3 \bar{h}\right\}\Psi_n^+ + \frac{i\epsilon}{4\bar{h}} \sum_{\substack{s\neq 0 \\ s\neq n}} (n+s)\,\Psi_s^+\,\Psi_{n-s}^+ \\
&+ \tfrac{1}{4}i\Psi_n^- \left\{(n - p\Lambda_h)\frac{H_p}{\bar{h}} \exp\left[-i(2n - p\Lambda_h)\int \frac{1}{\bar{h}^{\frac{1}{2}}}\mathrm{d}x\right]\right. \\
&\left. - q\Lambda_b \frac{B_q}{\bar{b}} \exp\left[-i(2n - q\Lambda_b)\int \frac{1}{\bar{h}^{\frac{1}{2}}}\mathrm{d}x\right]\right\} = O(\epsilon^2, \epsilon\mu^2, \mu^4),
\end{aligned} \tag{3.13}$$

and

$$\bar{h}^{\frac{1}{2}}\frac{\mathrm{d}\Psi_n^-}{\mathrm{d}x}+\left\{\frac{1}{2}\left(\frac{\mathrm{d}\bar{h}^{\frac{1}{2}}}{\mathrm{d}x}+\frac{\bar{h}^{\frac{1}{2}}}{\bar{b}}\frac{\mathrm{d}\bar{b}}{\mathrm{d}x}\right)+\tfrac{1}{6}\mathrm{i}\mu^2n^3\bar{h}\right\}\Psi_n^- -\frac{\mathrm{i}\epsilon}{4\bar{h}}\sum_{\substack{s\neq 0\\ s\neq n}}(n+s)\,\Psi_s^-\,\Psi_{n-s}^-$$
$$-\tfrac{1}{4}\mathrm{i}\Psi_n^+\left\{(n-p\Lambda_h)\frac{H_{-p}}{\bar{h}}\exp\left[\mathrm{i}(2n-p\Lambda_h)\int\frac{1}{\bar{h}^{\frac{1}{2}}}\mathrm{d}x\right]\right.$$
$$\left.-q\Lambda_b\frac{B_{-q}}{\bar{b}}\exp\left[\mathrm{i}(2n-q\Lambda_b)\int\frac{1}{\bar{h}^{\frac{1}{2}}}\mathrm{d}x\right]\right\}=O(\epsilon^2,\epsilon\mu^2,\mu^4). \tag{3.14}$$

Note that for the $n$th harmonics, $p$ and $q$ are chosen such that $(2n-p\Lambda_h)$ and $(2n-q\Lambda_b)$ are minimized. This ensures that the last term in (3.13) and (3.14) is a slowly varying function.

By introducing the following transform:

$$\Psi_n^{\pm}=A_n^{\pm}\exp\left[\pm\tfrac{1}{6}\mathrm{i}\mu^2n^3\int\bar{h}^{\frac{1}{2}}\mathrm{d}x\right], \tag{3.15}$$

(3.13) and (3.14) can be rewritten in terms of $A_n^{\pm}$ as

$$\bar{h}^{\frac{1}{2}}\frac{\mathrm{d}A_n^+}{\mathrm{d}x}+\frac{1}{2}\left(\frac{\mathrm{d}\bar{h}^{\frac{1}{2}}}{\mathrm{d}x}+\frac{\bar{h}^{\frac{1}{2}}}{\bar{b}}\frac{\mathrm{d}\bar{b}}{\mathrm{d}x}\right)A_n^+ +\frac{\mathrm{i}\epsilon}{4\bar{h}}\sum_{\substack{s\neq 0\\ s\neq n}}(n+s)\,A_s^+\,A_{n-s}^+\,\mathrm{e}^{-\mathrm{i}\Delta\alpha_{ns}x}$$
$$+\tfrac{1}{4}\mathrm{i}A_n^-\left\{(n-p\Lambda_h)\frac{H_p}{\bar{h}}\,\mathrm{e}^{-\mathrm{i}\Delta\beta_{np}x}-q\Lambda_b\frac{B_q}{\bar{b}}\,\mathrm{e}^{-\mathrm{i}\Delta\gamma_{nq}x}\right\}=O(\epsilon^2,\epsilon\mu^2,\mu^4), \tag{3.16a}$$

$$\bar{h}^{\frac{1}{2}}\frac{\mathrm{d}A_n^-}{\mathrm{d}x}+\frac{1}{2}\left(\frac{\mathrm{d}\bar{h}^{\frac{1}{2}}}{\mathrm{d}x}+\frac{\bar{h}^{\frac{1}{2}}}{\bar{b}}\frac{\mathrm{d}\bar{b}}{\mathrm{d}x}\right)A_n^- -\frac{\mathrm{i}\epsilon}{4\bar{h}}\sum_{\substack{s\neq 0\\ s\neq n}}(n+s)\,A_s^-\,A_{n-s}^-\,\mathrm{e}^{\mathrm{i}\Delta\alpha_{ns}x}$$
$$-\tfrac{1}{4}\mathrm{i}A_n^+\left\{(n-p\Lambda_h)\frac{H_{-p}}{\bar{h}}\,\mathrm{e}^{\mathrm{i}\Delta\beta_{np}x}-q\Lambda_b\frac{B_{-q}}{\bar{b}}\,\mathrm{e}^{\mathrm{i}\Delta\gamma_{nq}x}\right\}=O(\epsilon^2,\epsilon\mu^2,\mu^4), \tag{3.16b}$$

where

$$\Delta\alpha_{ns}=\tfrac{1}{2}\mu^2ns(n-s)\frac{1}{x}\int\frac{1}{\bar{h}^{\frac{1}{2}}}\mathrm{d}x, \tag{3.17a}$$

$$\Delta\beta_{np}=\frac{1}{x}\int\frac{1}{\bar{h}^{\frac{1}{2}}}(2n-p\Lambda_h+\tfrac{1}{3}\mu^2n^3\bar{h})\,\mathrm{d}x, \tag{3.17b}$$

$$\Delta\gamma_{nq}=\frac{1}{x}\int\frac{1}{\bar{h}^{\frac{1}{2}}}(2n-q\Lambda_b+\tfrac{1}{3}\mu^2n^3\bar{h})\,\mathrm{d}x. \tag{3.17c}$$

In the above equations $\Delta\alpha_{ns}$ denotes a detuning factor which is a phase mismatching between different harmonics propagating in a same direction. $\Delta\beta_{np}$ and $\Delta\gamma_{nq}$ represent detuning factors resulting from the slight deviations in the incident wavenumbers from the Bragg wavenumber. We remark here that (3.16$a$ and $b$) are valid only near resonance such that all the detuning factors are of the magnitude of $O(\mu^2)$. If the incident waves satisfy the Bragg reflection condition, $\Delta\beta_{np}$ and $\Delta\gamma_{nq}$ are zero. In this case (3.15) and (3.16) are equivalent to those obtained by Lau & Barcilon (1972) for a constant channel width.

If, for simplicity, there is no phase difference between the undulations $\tilde{h}$ and $\tilde{b}$, (3.16$a$, $b$) become

$$\bar{h}^{\frac{1}{2}}\frac{\mathrm{d}A_n^+}{\mathrm{d}x}+\frac{1}{2}\left(\frac{\mathrm{d}\bar{h}^{\frac{1}{2}}}{\mathrm{d}x}+\frac{\bar{h}^{\frac{1}{2}}}{\bar{b}}\frac{\mathrm{d}\bar{b}}{\mathrm{d}x}\right)A_n^+ +\frac{\mathrm{i}\epsilon}{4\bar{h}}\sum_{\substack{s\neq 0\\ s\neq n}}(n+s)\,A_s^+\,A_{n-s}^+\,\mathrm{e}^{-\mathrm{i}\Delta\alpha_{ns}x}$$
$$+\mathrm{i}A_n^-\Delta nm\,\mathrm{e}^{-\mathrm{i}\Delta\beta_{nm}x}=O(\epsilon^2,\epsilon\mu^2,\mu^2), \tag{3.18}$$

$$\bar{h}^{\frac{1}{2}}\frac{\mathrm{d}A_n^-}{\mathrm{d}x}+\frac{1}{2}\left(\frac{\mathrm{d}\bar{h}^{\frac{1}{2}}}{\mathrm{d}x}+\frac{\bar{h}^{\frac{1}{2}}}{\bar{b}}\frac{\mathrm{d}\bar{b}}{\mathrm{d}x}\right)A_n^- - \frac{\mathrm{i}\epsilon}{4\bar{h}}\sum_{\substack{s\neq 0\\ s\neq n}}(n+s)\,A_s^-\,A_{n-s}^-\,\mathrm{e}^{\mathrm{i}\Delta\alpha_{ns}x}$$
$$-\mathrm{i}A_n^+\,\Delta_{nm}^*\,\mathrm{e}^{\mathrm{i}\Delta\beta_{nm}x}=O(\epsilon^2,\epsilon\mu^2,\mu^2) \quad (3.19)$$

where
$$\Delta_{nm}=\frac{1}{4}\left\{(n-m\Lambda)\frac{H_m}{\bar{h}}-m\Lambda\frac{B_m}{\bar{b}}\right\}, \quad (3.20a)$$

$$\Delta\beta_{nm}=\frac{1}{x}\int\frac{1}{\bar{h}^{\frac{1}{2}}}(2n-m\Lambda+\tfrac{1}{3}\mu^2n^3\bar{h})\,\mathrm{d}x, \quad (3.20b)$$

and $\Delta_{nm}^*$ is the complex conjugate of $\Delta_{nm}$.

### 3.2. *Analytical solutions for linear problems*

In this section, we consider the linear problems with a simplified geometry where the mean depth and the mean width are constants; i.e. $\bar{h}=1$ and $\bar{b}=$ constant. The linearized governing equations become

$$\frac{\mathrm{d}A_n^+}{\mathrm{d}x}+\mathrm{i}A_n^-\,\Delta_{nm}\,\mathrm{e}^{-\mathrm{i}\Delta\beta_{nm}x}=0, \quad (3.21)$$

$$\frac{\mathrm{d}A_n^-}{\mathrm{d}x}-\mathrm{i}A_n^+\,\Delta_{nm}^*\,\mathrm{e}^{\mathrm{i}\Delta\beta_{nm}x}=0, \quad (3.22)$$

where $\Delta_{nm}$ and $\Delta\beta_{nm}$ are reduced to

$$\Delta_{nm}=\frac{1}{4}\left\{(n-m\Lambda)\,H_m-m\Lambda\frac{B_m}{\bar{b}}\right\}, \quad (3.23a)$$

$$\Delta\beta_{nm}=(2n-m\Lambda+\tfrac{1}{3}\mu^2n^3). \quad (3.23b)$$

These equations can be viewed as the shallow-water limit of the linear theory developed by Liu (1987). In the case of a channel with a constant width ($B_m=0$), these equations recover Mei's (1985) linear theory in the shallow-water limit.

Consider the case where the undulation is confined within a finite region, $0<x<L$, and the incident wavetrain is arriving from $x\sim-\infty$. There is no reflected wave from $x\sim\infty$. Equations (3.21) and (3.22) have the following analytic solution:

$$\frac{A_n^+(x)}{A_n^+(0)}=\exp\left[-\mathrm{i}(\tfrac{1}{2}\Delta\beta_{nm})\,x\right]\frac{s\cosh s(L-x)-\mathrm{i}\tfrac{1}{2}\Delta\beta_{nm}\sinh s(L-x)}{s\cosh sL-\mathrm{i}\tfrac{1}{2}\Delta\beta_{nm}\sinh sL}, \quad (3.24)$$

$$\frac{A_n^-(x)}{A_n^+(0)}=\exp\left[\mathrm{i}(\tfrac{1}{2}\Delta\beta_{nm})\,x\right]\frac{-\mathrm{i}\Delta_{nm}^*\sinh s(L-x)}{s\cosh sL-\mathrm{i}\tfrac{1}{2}\Delta\beta_{nm}\sinh sL}, \quad (3.25)$$

where
$$s^2=|\Delta_{nm}|^2-(\tfrac{1}{2}\Delta\beta_{nm})^2, \quad (3.26)$$

and $A_n^+(0)$ are the incident wave amplitudes of the $n$th harmonic at $x=0$. The energy conservation requirement is satisfied by (3.24) and (3.25); i.e. $|A_n^+(x)/A_n^+(0)|^2+|A_n^-(x)/A_n^+(0)|^2=1$.

## 4. Numerical solutions in a channel with a constant width

Since there is no general analytical solution for nonlinear equations (3.18) and (3.19), a numerical integration scheme must be employed to solve a specific problem. As a particular set of examples, we consider the shallow-water wavetrain propagating over a ripple patch in a channel with a constant mean depth and a constant width.

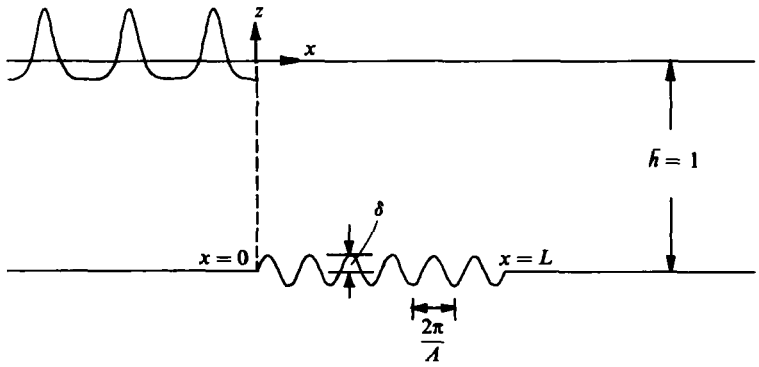


FIGURE 1. Definition sketch.

From (3.18) and (3.19), the governing equations can be reduced to

$$\frac{dA_n^+}{dx}+\tfrac{1}{4}i\epsilon \sum_{\substack{s\neq 0\\ s\neq n}} (n+s)\,A_s^+ A_{n-s}^+ e^{-i\Delta\alpha_{ns}x}+iA_n^- \Delta_{nm} e^{-i\Delta\beta_{nm}x} = O(\epsilon^2), \tag{4.1}$$

$$\frac{dA_n^-}{dx}-\tfrac{1}{4}i\epsilon \sum_{\substack{s\neq 0\\ s\neq n}} (n+s)\,A_s^- A_{n-s}^- e^{i\Delta\alpha_{ns}x}-iA_n^+ \Delta_{nm}^* e^{i\Delta\beta_{nm}x} = O(\epsilon^2), \tag{4.2}$$

where

$$\Delta\beta_{nm} = 2n-m\Lambda+\tfrac{1}{3}\mu^2 n^3, \tag{4.3a}$$

$$\Delta_{nm} = -\tfrac{1}{4}nH_m+O(\epsilon^2). \tag{4.3b}$$

Here $O(\epsilon^2)$ is the abbreviation for $O(\epsilon^2, \epsilon\mu^2, \mu^4)$. The rippled bed has only one wavenumber satisfying the Bragg reflection condition associated with the first harmonic of the incident wavetrain. As shown in figure 1, the water depth is assumed to be

$$h = 1-\delta\sin\Lambda x = 1+\tfrac{1}{2}i\delta\,(e^{i\Lambda x}-e^{-i\Lambda x}), \tag{4.4}$$

$$\left.\begin{aligned} \Lambda &= 2+\tfrac{1}{3}\mu^2-\Delta\beta_{11}, \quad \Delta_{11} = -\tfrac{1}{4}i\delta,\\ \Delta\beta_{nm} &= \Delta_{nm} = 0, \quad \text{if } |n|\neq 1, |m|\neq 1, \end{aligned}\right\} \tag{4.5}$$

where the real quantity $\delta$ represents the $O(\epsilon)$ amplitude of the depth undulations.

### 4.1. *Propagation and reflection of a modulated wavetrain*

The first example examined here concerns the resonant reflection of a modulated wavetrain over a rippled bed in an otherwise constant depth. This problem was first studied by Lau & Barcilon (1972) using two harmonics. Their governing equations for the transmitted and reflected wave fields are different from (4.1) and (4.2).

To ensure the accuracy of the numerical scheme used for integrating (4.1) and (4.2), we first obtained numerical solutions for a shallow-water harmonic-generation problem in a constant depth and compared the numerical solutions with experimental data by Goda (1967). Since the reflection is absent, the governing equation (4.1) becomes

$$\frac{dA_n^+}{dx}+\tfrac{1}{4}i\epsilon \sum_{\substack{s\neq 0\\ s\neq n}} (n+s)\,A_s^+ A_{n-s}^+ e^{-i\Delta\alpha_{ns}x} = 0. \tag{4.6}$$

The fourth-order Runge–Kutta method is employed to integrate (4.6) with boundary conditions $A_1^+(0) = 1$ and $A_n^+(0) = 0$ for $n \neq 1$.

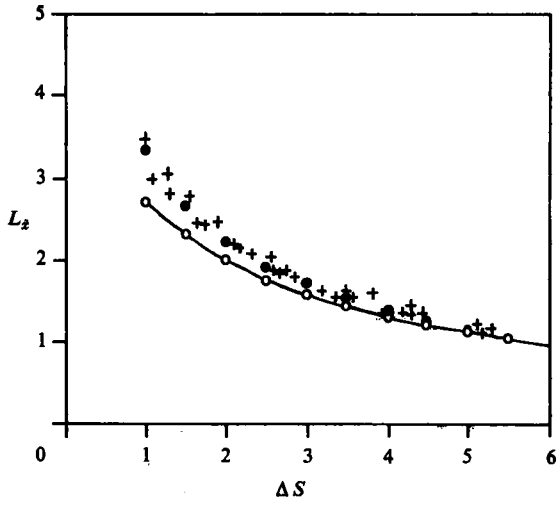


FIGURE 2. Beat length $L_{\tilde{x}}$ *vs.* mismatch parameter $\Delta S$. ——, theory by Mei & Ünlüata (1972); + + +, laboratory data from Goda (1967); ○○○, numerical result using 2 harmonics; ●●●, numerical result using 5 harmonics.

Numerical solutions for using two harmonics ($n = 2$) and five harmonics ($n = 5$) are obtained and plotted in figure 2 for the beat length of the second harmonic *vs.* the phase mismatch parameter $\Delta S$. The beat length $L_{\tilde{x}}$ is defined as the distance between two successive second-harmonic wave crests; the phase mismatch parameter measures the relative importance of the nonlinearity and the dispersion, i.e.

$$\Delta S = \frac{4\mu^2}{3\epsilon}. \tag{4.7}$$

As shown in figure 2, the numerical solutions with two harmonics agree very well with Mei & Ünlüata's (1972) analytical solutions. In the region of smaller $\Delta S$ (the nonlinearity becomes more important), numerical solutions with five harmonics yield better agreement with Goda's data. As $\Delta S$ becomes even smaller, more harmonics should be included in the analysis. Indeed, in a related work Bryant (1973) has made more accurate computations by including 11 harmonics in the coupled equations derived from the KdV equations. Other related experimental and theoretical work concerning the higher-harmonic generation in shallow water can be found in Boczar-Karakiewicz (1972) and Paplinska, Rugeland & Werner (1983).

From the evidence of the previous example, the fourth-order Runge–Kutta method is a suitable scheme for solving the simultaneous nonlinear ordinary differential equation (4.6). To include the reflected wave field $A_n^-$ in the analysis, the scheme must be modified. Liu & Tsay (1983) developed an iteration scheme to solve the coupled equations similar to (4.1) and (4.2). They first solved the transmitted wave field, i.e. $A_n^+$, in (4.1) by ignoring the reflected wave field entirely. Once the approximated transmitted wave field is obtained, the reflected wave field is calculated from (4.2) treating the $A_n^+$ as known quantities. The newly obtained values of $A_n^-$ are used in (4.1) to find the corrected transmitted wave field. The procedure is repeated until converged solutions are obtained. Provided that the reflected wave intensity is weak, Liu & Tsay's (1983) iteration scheme converges and yields accurate solutions. In the present study, the reflection is strong because of resonance. The iteration scheme can

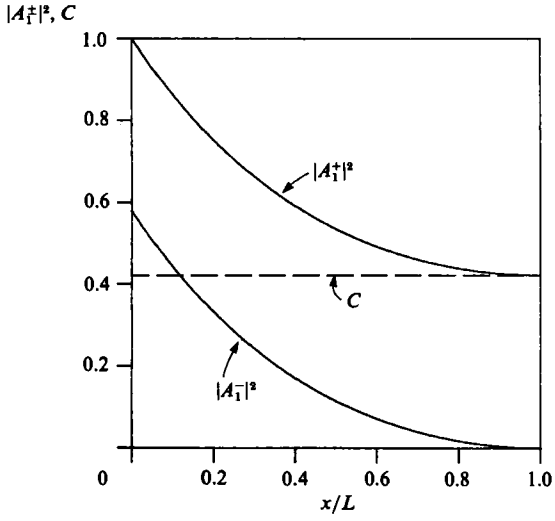


FIGURE 3. Transmission intensity $|A_1^+|^2$, reflection intensity $|A_1^-|^2$ and integration constant $C$ (0.4298) of modulated wave from linear theory. $\epsilon = 0$, $l = 15.15$, $\delta = 0.264$ and $A_1^+(0) = 1$.

still be successful if we increase the amplitude of the topographical undulations gradually from zero to the desired value during the iterative procedure.

Numerical solutions are obtained for the transmitted and reflected wave fields over a rippled bed described in figure 1 and (4.4). Focusing on the resonance case, we use the following parameters, which are equivalent to those used by Lau & Barcilon (1972):

$$\left.\begin{aligned} &\Delta\beta_{11} = 0, \quad A_1^+(0) = 1, \quad A_n^+(0) = 0 \quad \text{if } |n| \neq 1, \\ &\Delta S = 0.3, \quad \delta = 3\epsilon, \quad l = \frac{4}{3\epsilon}, \end{aligned}\right\} \tag{4.8}$$

where $l$ is called the interaction length (Armstrong *et al.* 1962) in nonlinear optics. The interaction length is defined as the distance, along the path of the modulating shallow-water wave in a constant depth, from the point where the second-harmonic-wave energy intensity is zero to the point where the second-harmonic wave component has gained about 75% of the wave energy from the first harmonic. To compare our solutions with Lau & Barcilon's (1972) results, we use the following numerical values of parameters: $\epsilon = 0.088$, then $\mu^2 = 0.0198$, $\delta = 0.264$, and $l = 15.15$. The length of the rippled bed $L$ is chosen to be the same as the interaction distance $l$ (Lau & Barcilon 1972). As indicated in (4.18), and the starting point of the rippled bed, $x = 0$ coincides with the crest of the first harmonic.

To verify the present iterative numerical scheme, we obtained numerical solutions for the linear problems and compared them to the analytical solutions given in (3.24) and (3.25). Numerical results coincide with the analytical solutions almost perfectly. The transmitted and reflected wave intensities over the rippled bed are plotted in figure 3. The difference between the analytical and numerical results is not visible. The maximum reflection, which occurs at the front of the rippled bed, is 0.76. Because of the conservation of wave energy, the following is true (Lau & Barcilon 1972):

$$\sum_n |A_n^+|^2 - \sum_n |A_n^-|^2 = C, \tag{4.9}$$

where $C$ is a constant, which is satisfied by the numerical results shown in figure 4.

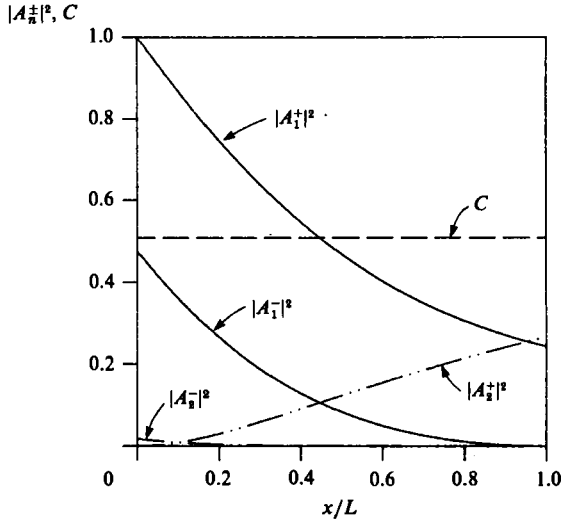


FIGURE 4. Transmission intensities $|A_n^+|^2$, reflection intensities $|A_n^-|^2$ and integration constant $C$ (0.5079) of modulated wave from nonlinear theory using 2 harmonics. $\Delta S = 0.3$, $l = 15.15$, $\delta = 0.264$, $A_1^+(0) = 1$ and $A_n^+(0) = 0$ if $|n| \neq 1$.

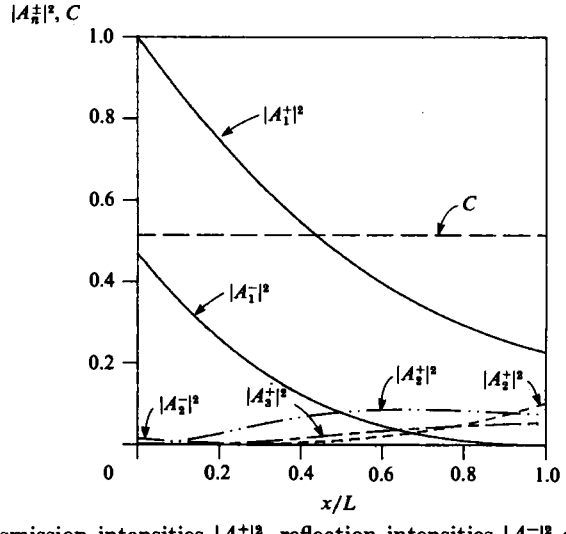


FIGURE 5. Transmission intensities $|A_n^+|^2$, reflection intensities $|A_n^-|^2$ and integration constant $C$ (0.5144) of modulated wave from nonlinear theory using 5 harmonics (see figure 4 for parameters).

Numerical results based on the nonlinear theory are obtained for two cases: two harmonics and five harmonics. The wave-harmonic intensities for each case are shown in figures 4 and 5 respectively. If the reflection coefficient $R$ is defined as

$$R = \left( \frac{\sum_n |A_n^-|^2}{\sum_n |A_n^+|^2} \right)^{\frac{1}{2}}, \quad \text{at } x = 0. \tag{4.10}$$

the reflection coefficient for both cases is 0.6. The inclusion of higher harmonics does not affect the reflection coefficient significantly. On the other hand, the reflection

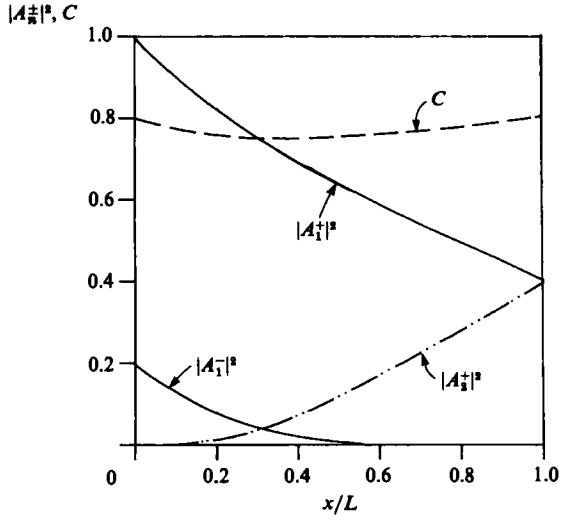


FIGURE 6. Transmission intensities $|A_n^+|^2$, reflection intensities $|A_n^-|^2$ and integration constant $C$ by Lau & Barcilon (1972) (see figure 4 for parameters).

coefficient is over-estimated by the linear theory, which ignores the energy transfer from the lower harmonics to higher harmonics through nonlinearity.

Lau & Barcilon (1972) studied the same problem, including only two harmonics. Their numerical solutions showed smaller reflected wave intensities; the reflection coefficient was 0.46. We discovered, however, that their numerical results do not satisfy the conservation of energy; their $C$-value is not a constant over the rippled bed. For comparison, we have replotted their results in figure 6, using our notation. As indicated in figures 4 and 5, our numerical solutions give constant $C$-values for cases with both two and five harmonics.

The effects of the detuning factor $\Delta\beta_{11}$ on the reflection are examined next. Using $\epsilon = 0.0881$, $\mu^2 = 0.1067$, $\delta = 0.2$ and $L = 10\pi$, we calculated the transmitted and reflected wave fields for different values of $\Delta\beta_{11} L$. Five harmonics are kept in the computations. The reflected wave intensities at the beginning point of the rippled bed ($x = 0$) are plotted in figure 7. The analytical solutions (3.25) based on the linear theory are also shown for comparison. The linear theory presents a symmetric curve with respect to the resonance condition ($\Delta\beta_{11} L = 0$). The nonlinear solutions are skewed with the maximum reflection intensity at $\Delta\beta_{11} \mathrm{L} = 1.75$. It is also noticeable that the nonlinearity reduces not only the maximum reflection but also the range of $\Delta\beta_{11} L$ within which the reflection is significant.

### 4.2. *Reflection of a cnoidal wave*

The cnoidal wave, propagating in a constant water depth without changing its shape, can be expressed in the Fourier series shown in (2.7$a$). According to Miles (1976) and Sarpkaya & Isaacson (1981) the amplitude of each harmonic is found to be

$$A'_n = \tfrac{8}{3} k'^2 h_0'^3 n r^n (1 - r^{2n})^{-1}, \quad n = 1, 2, \ldots, \tag{4.11}$$

where $A'_n$ is the amplitude of the $n$th harmonic, $k'$ is the wavenumber of the first harmonic, $h'_0$ is the water depth and $r$ is given by the equation

$$r = \exp\left\{\frac{-\pi K(\bar{\kappa})}{K(\kappa)}\right\}. \tag{4.12}$$

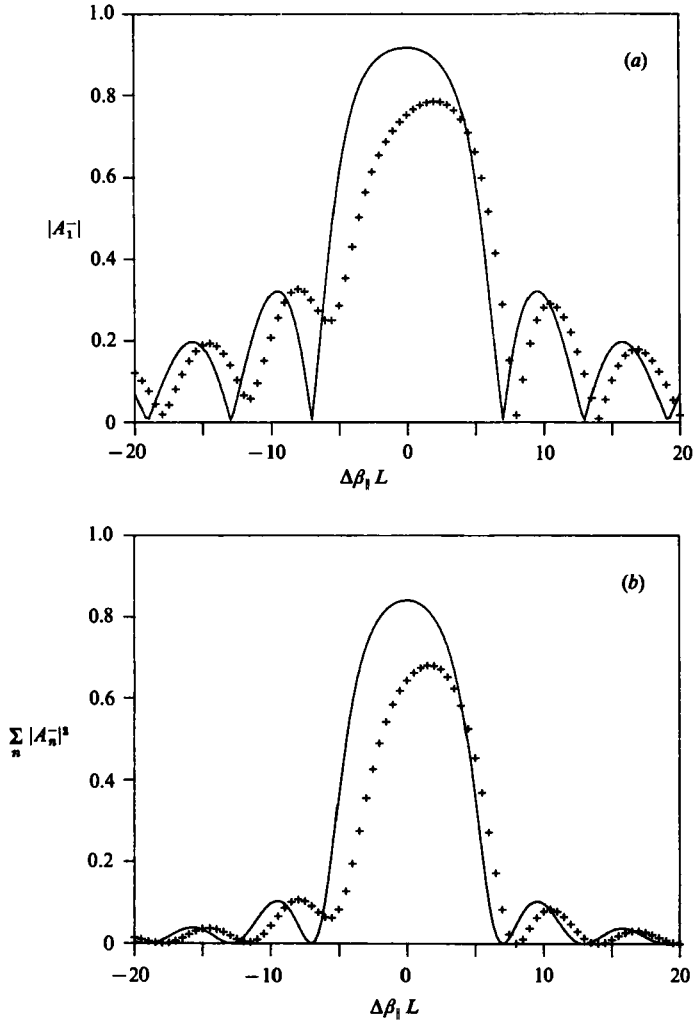


FIGURE 7. (*a*) Reflected first-harmonic amplitude $|A_1^-|$, and (*b*) reflection intensity $\Sigma_n |A_n^-|^2$ of modulated wave. ——, linear theory; + + +, nonlinear theory using 5 harmonics. $\epsilon = 0.0881$, $\mu^2 = 0.1067$, $\delta = 0.2$, $L = 10\pi$, $A_1^+(0) = 1$ and $A_n^+(0) = 0$ if $|n| = 1$.

Here $K$ is the complete elliptic integral of the first kind, $\kappa$ is the modulus and $\bar{\kappa}\,(= (1-\kappa^2)^{\frac{1}{2}})$ is the complementary modulus. $\kappa$ is uniquely related to wave height $H'$, water depth $h_0'$, and wavenumber $k'$, by

$$\frac{H'/h_0'}{(k'h_0')^2} = \frac{4}{3\pi^2}\kappa^2 K(\kappa). \tag{4.13}$$

All the quantities with a prime are dimensional ones. Introducing the characteristic wave amplitude $a_0'$ as

$$a_0' = \left(\sum_n A_n'^2\right)^{\frac{1}{2}}, \quad n = 1, 2, \ldots, \tag{4.14}$$

we define the normalized wave amplitude $A_n$ by

$$A_n = \frac{A_n'}{a_0'}, \quad A_{-n} = A_n. \tag{4.15}$$

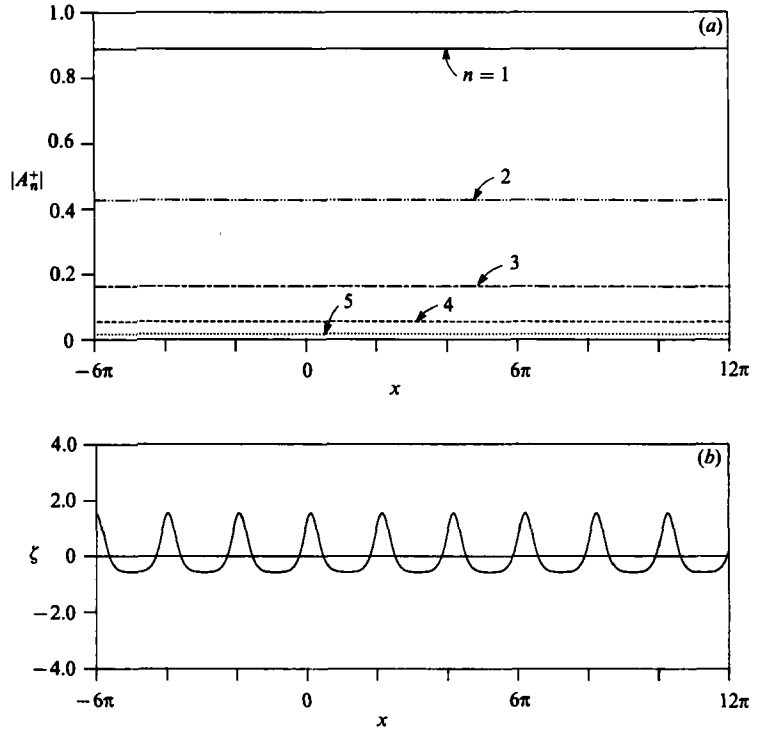


FIGURE 8. (*a*) Wave amplitude $|A_n^+|$ of a cnoidal wave propagating on a flat bottom from nonlinear theory using 5 harmonics; ——, $n = 1$; —··—, 2; ———, 3; – – –, 4; ·····, 5; and (*b*) corresponding free-surface displacement $\zeta$ at $t = 0$.

To demonstrate that the present model can simulate approximately the propagation of a cnoidal wave, we choose $H' = 2$ m, $h_0' = 10$ m and $\omega' = 0.3234$ rad/s. The other dimensional parameters are $A_1' = 0.7864$ m, $A_2' = 0.370$ m, $A_3' = 0.1382$ m, $A_4' = 0.0460$ m, $A_5' = 0.0144$ m, $a_0' = 0.8813$ m. The corresponding dimensionless parameters become $A_1 = 0.8923$, $A_2 = 0.4198$, $A_3 = 0.1568$, $A_4 = 0.0522$, $A_5 = 0.0163$, $\epsilon = 0.0881$, and $\mu^2 = 0.1067$. We have ignored the higher harmonics ($n \geqslant 6$) whose amplitudes are smaller than 0.55 % of that of the first harmonic. Using these parameters as initial conditions, (4.1) is solved numerically for the transmitted wave field only; i.e. $A_n^- \equiv 0$. The water depth is constant ($h = 1$ and $\delta = 0$), and the computations are performed between $-6\pi \leqslant x \leqslant 12\pi$. Numerical results for the free-surface profile and the wave amplitude for each harmonic are shown in figure 8. If the theory were without approximations, the amplitude distribution for each harmonic should have been uniform. The variations in our numerical results are, however, quite small and the free-surface profile appears to remain in the same shape.

To investigate the resonant reflection of cnoidal waves from the rippled bed we place the rippled bed along $0 \leqslant x \leqslant 6\pi$. The wavenumber of the ripples satisfies the Bragg reflection condition associated with the first harmonic of the cnoidal wave (i.e. $\Lambda = 2 + \frac{1}{3}\mu^2$ and $\Delta\beta_{11} = 0$). Using $\delta = 0.2$, the transmitted and reflected wave amplitudes and the corresponding free-surface displacement at $t = 0$ are plotted in figure 9(*a*, *b*, *c*) respectively. For comparison, linear solutions with $\epsilon = 0$ are also shown in figure 10(*a*–*c*) although, strictly speaking, a linear theory is not valid in this case. In the linear case only the first harmonic is affected by the rippled bed

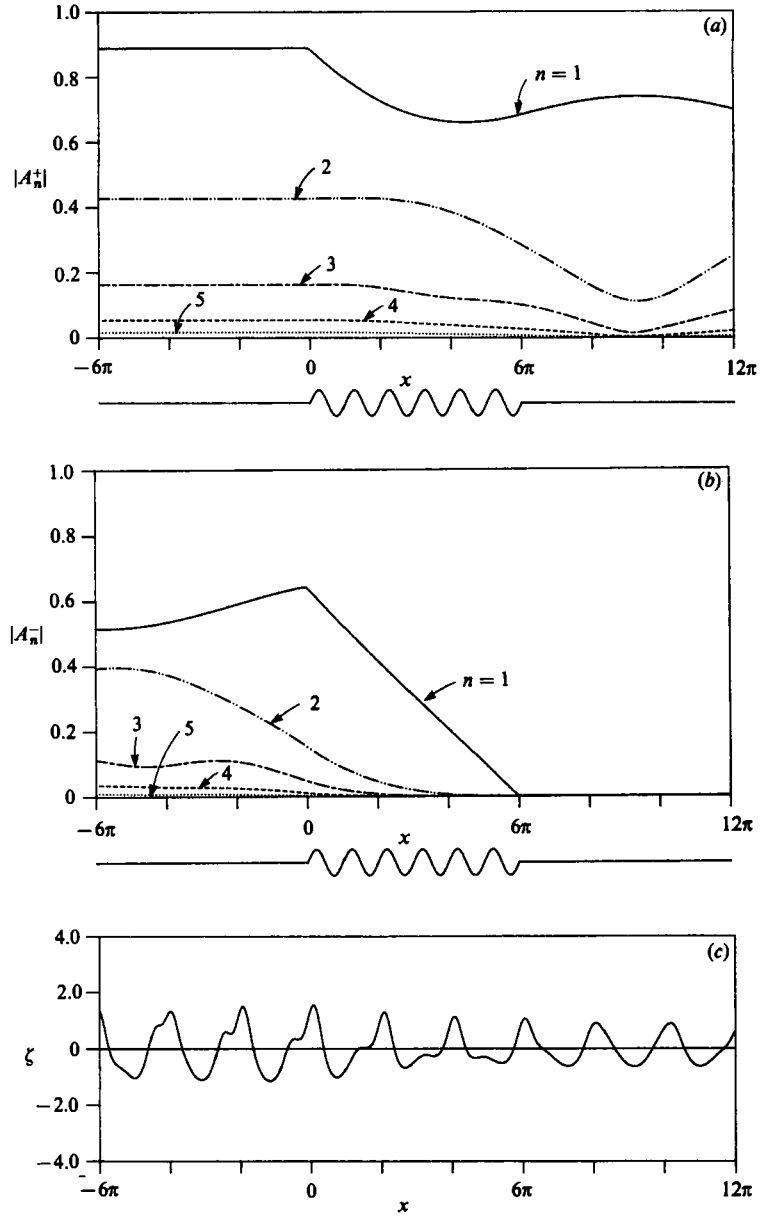


FIGURE 9. (*a*) Transmitted wave amplitude $|A_n^+|$, (*b*) reflected wave amplitude $|A_n^-|$ of uniform cnoidal wave from nonlinear theory using 5 harmonics; ——, $n = 1$; —··—, 2; — — —, 3; – – –, 4; ·····, 5; and (*c*) free-surface displacement $\zeta$ at $t = 0$.

(figure 10*a*). The nonlinearity, however, transfers a certain amount of wave energy from the higher harmonics to the first harmonic. As a result, the reflected first-harmonic wave intensity predicted by the nonlinear theory over the rippled bed is slightly higher than that suggested by the linear theory.

In front of the rippled bed ($x \leqslant 0$), the linear theory predicts uniform reflected wave amplitude. The nonlinear theory indicates that the amplitude of the first harmonic

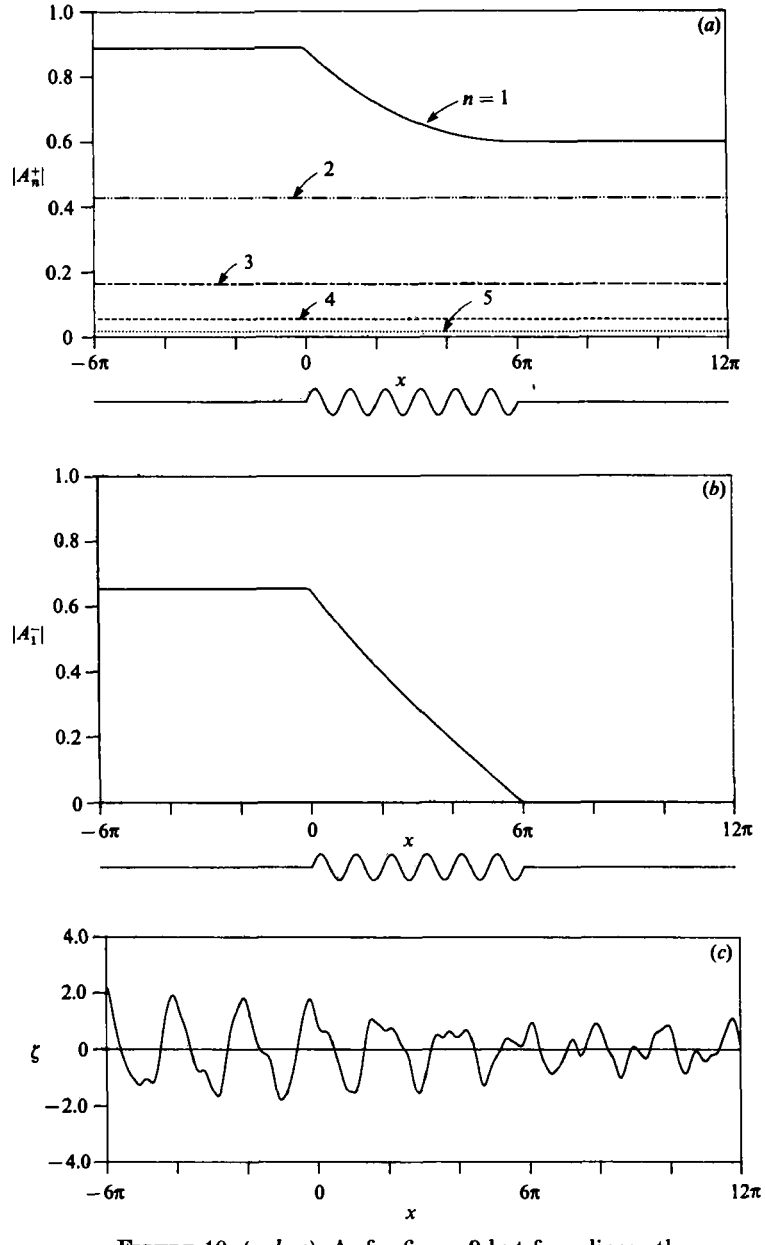


FIGURE 10. (*a*, *b*, *c*). As for figure 9 but from linear theory.

decreases as the reflected wave propagates upstream. This is caused by the energy transfer to higher harmonics. To highlight this point, we have replotted $|A_1^-|$ from linear and nonlinear theories together in figure 11.

After the cnoidal waves pass the rippled-bed patch, the permanent shape degenerates because of the imbalance of energy among harmonics (figure 9*c*).

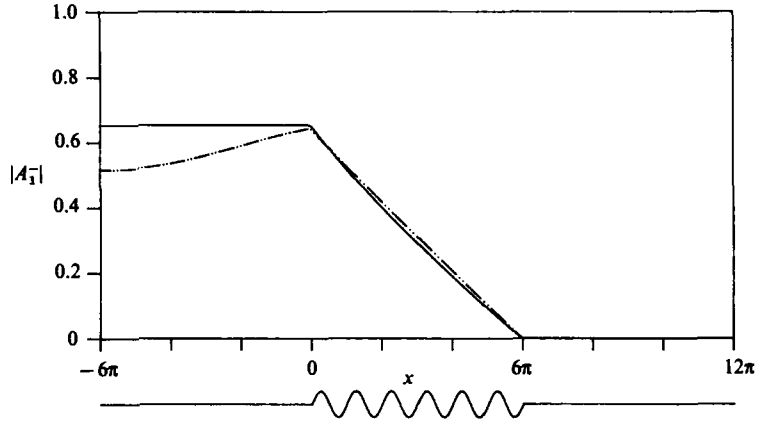


FIGURE 11. Comparison of reflected first harmonic amplitude $|A_1^-|$ from linear and nonlinear results; ——, linear; —· ·—, nonlinear.

## 5. Discussion and concluding remarks

In this paper we have studied the propagation of a shallow-water wave in a constant depth and the resonant reflection from corrugated boundaries.

In deriving the governing equations we neglected energy dissipation. A simple linear energy-dissipation model can be included in the governing equations and is given in the Appendix. No attempt has been made to solve the two-dimensional equation (2.16), which includes refraction and diffraction effects; numerical solutions of (2.16) are straightforward.

The effects of nonlinearity on the reflection of shallow-water waves have been investigated for the case of a constant mean depth. Depending on the incident wave conditions, the nonlinearity affects the reflection in different ways. For the reflection of cnoidal waves nonlinearity causes stronger reflection of the first-harmonic wave component over the rippled patch than that predicted by linear theory. As the reflected waves propagate upstream, the wave intensity of the reflected first-harmonic waves decreases because of the energy transfer between harmonics. On the other hand, for the modulated incident wavetrain calculated herein nonlinearity causes weaker reflection of the first harmonic than that predicted by the linear theory owing to the partitioning of energy between reflected and transmitted higher harmonics generated over the rippled patch. These results might be changed for different boundary conditions at the beginning of the rippled bed.

The combined effects of the detuning factor $\Delta\beta_{11}$ and nonlinearity reduce the reflection. Linear theory gives a symmetric reflection curve about the Bragg condition ($\Delta\beta_{11} = 0$), while nonlinear theory predicts a skewed one. Nonlinearity reduces the maximum value of reflection and shifts the maximum to the positive side of $\Delta\beta_{11}$. As reported by Davies (1982), the shifting of the maximum reflection could also be influenced by the number of ripples on the bed. Owing to the lack of experimental data in shallow water, we show only the general trends involved in nonlinearity. Careful experiments would be valuable to confirm the present study.

The research reported here is supported by the New York Sea Grant Institute. Conversations with Dr J. T. Kirby have been fruitful. His willingness in sharing the draft of Vengayil's thesis is appreciated and acknowledged. Comments made by referees have also been helpful in the presentation of this paper.

## Appendix

The Boussinesq equations (2.1) and (2.2) can be modified to include an energy-dissipation term due to either a laminar viscous boundary layer or turbulent bottom friction. The momentum equation (2.6) can be rewritten as

$$\frac{\partial \boldsymbol{u}}{\partial t}+\epsilon \boldsymbol{u}\cdot\boldsymbol{\nabla}\boldsymbol{u}+\boldsymbol{\nabla}\zeta+w\boldsymbol{u}=\tfrac{1}{3}\mu^2\bar{h}^2\,\boldsymbol{\nabla}\left(\boldsymbol{\nabla}\cdot\frac{\partial \boldsymbol{u}}{\partial t}\right)+O(\epsilon^2), \tag{A 1}$$

where $w(x,y)$ is an energy dissipation coefficient and is assumed to be $O(\epsilon)$. The continuity equation remains the same as (2.1).

For the periodic motion in time we propose that

$$w\boldsymbol{u}=\tfrac{1}{2}\sum_n W_n\,\boldsymbol{U}_n\,\mathrm{e}^{-\mathrm{i}nt}. \tag{A 2}$$

Substituting (2.7$a$, $b$) and (A 2) into (A 1) and collecting Fourier components, we obtain

$$-\mathrm{i}(n+\mathrm{i}W_n)\,\boldsymbol{U}_n+\tfrac{1}{2}\epsilon\sum_s \boldsymbol{U}_s\cdot\boldsymbol{\nabla}\boldsymbol{U}_{n-s}+\boldsymbol{\nabla}\zeta_n=\tfrac{1}{3}\mu^2n^2\bar{h}\,\boldsymbol{\nabla}\zeta_n+O(\epsilon^2), \tag{A 3}$$

where $|\boldsymbol{\nabla}W_n|\sim O(\epsilon^2)$ are assumed.

Following the same procedure as given in §2, we have

$$\boldsymbol{\nabla}\cdot(\bar{h}\boldsymbol{\nabla}\zeta_n)+\boldsymbol{\nabla}\tilde{h}\cdot\boldsymbol{\nabla}\zeta_n+n\left(n+\mathrm{i}W_n-\frac{n\tilde{h}}{\bar{h}}+\tfrac{1}{3}\mu^2n^3\bar{h}\right)\zeta_n$$
$$+\epsilon\sum_s\left[\tfrac{1}{2}\mathrm{i}n\boldsymbol{\nabla}\cdot(\zeta_s\,\boldsymbol{U}_{n-s})+\tfrac{1}{2}\bar{h}\boldsymbol{\nabla}\cdot(\boldsymbol{U}_s\cdot\boldsymbol{\nabla}\boldsymbol{U}_{n-s})\right]=O(\epsilon^2). \tag{A 4}$$

Upon ignoring $\tilde{h}$ and terms of the order of $\mu^2$ and $\epsilon$, and considering only the first harmonic, we simplify (A 4) and convert the resulting equation into the following form:

$$\boldsymbol{\nabla}'\cdot(gh'\boldsymbol{\nabla}'\zeta')+(\omega'^2+\mathrm{i}w'\omega')\,\zeta'=0. \tag{A 5}$$

This equation is the shallow-water limit of Booij's (1981) model. After introducing the slow scale in the lateral direction (A 4) is rewritten as

$$\bar{h}\nabla^2\zeta_n+\boldsymbol{\nabla}(\bar{h}+\tilde{h})\cdot\boldsymbol{\nabla}\zeta_n+n\left(n+\mathrm{i}W_n-\frac{n\tilde{h}}{\bar{h}}+\tfrac{1}{3}\mu^2n^3\bar{h}\right)\zeta_n$$
$$-\epsilon\sum_{\substack{s\neq0\\ s\neq n}}\left\{\frac{n^2-s^2}{2\bar{h}}\zeta_s\zeta_{n-s}-\frac{n+s}{2(n-s)}\frac{\partial\zeta_s}{\partial x}\frac{\partial\zeta_{n-s}}{\partial x}\right\}=O(\epsilon^2). \tag{A 6}$$

Equation (A 6), instead of (2.16), can be used as a governing equation. The energy dissipation coefficients for various cases are available from the work of Dalrymple, Kirby & Hwang (1984).

## REFERENCES


ARMSTRONG, J. A., BLOEMBERGEN, N., DUCUING, J. & PERSHAN, P. S. 1962 Interactions between light waves in a nonlinear dielectric. *Phys. Rev.* **127**, 1918–1939.

BOCZAR-KARAKIEWICZ, B. 1972 Transformation of wave profile in shallow water – a Fourier analysis. *Arch. Hydrotechniki* **19**, 197–210.

BOOIJ, N. 1981 Gravity waves on water with nonuniform depth and current. Ph.D. thesis (partial), Technical University of Delft, The Netherlands.

BRYANT, P. J. 1973 Periodic waves in shallow water. *J. Fluid Mech.* **59**, 625–644.

DALRYMPLE, R. A., KIRBY, J. T. & HWANG, P. A. 1984 Wave diffraction due to areas of energy dissipation. *J. Waterway, Port, Coastal & Ocean Engng Div. ASCE* **110**, 67–79.

DAVIES, A. G. 1982 The reflection of wave energy by undulations on the seabed. *Dyn. Atmos. Oceans* **6**, 207–232.

DAVIES, A. G. & HEATHERSHAW, A. D. 1984 Surface-wave propagation over sinusoidally varying topography. *J. Fluid Mech.* **144**, 419–443.

GODA, Y. 1967 Travelling secondary wave crests in wave channels. *Port and Harbour Research Institute*, Ministry of Transport, Japan 13, pp. 32–38.

KIRBY, J. T. 1986*a* A general wave equation for waves over rippled beds. *J. Fluid Mech.* **162**, 171–186.

KIRBY, J. T. 1986*b* On the gradual reflection of weakly nonlinear Stokes waves in regions with varying topography. *J. Fluid Mech.* **162**, 187–209.

LAU, J. & BARCILON, A. 1972 Harmonic generation of shallow water waves over topography. *J. Phys. Oceanogr.* **2**, 405–410.

LIU, P. L.-F. 1987 Resonant reflection of water waves in a long channel with corrugated boundaries. *J. Fluid Mech.* (In press.)

LIU, P. L.-F. & TSAY, T.-K. 1983 On weak reflection of water waves. *J. Fluid Mech.* **131**, 59–71.

LIU, P. L.-F., YOON, S. B. & KIRBY, J. T. 1985 Nonlinear refraction–diffraction of waves in shallow water. *J. Fluid Mech.* **153**, 184–201.

MEI, C. C. 1985 Resonant reflection of surface water waves by periodic sandbars. *J. Fluid Mech.* **152**, 315–335.

MEI, C. C. & ÜNLÜATA, U. 1972 Harmonic generation in shallow water waves. In *Waves on Beaches* (ed. R. E. Meyer), pp. 181–202. Academic.

MILES, J. W. 1976 Damping of weakly nonlinear shallow-water waves. *J. Fluid Mech.* **76**, 251–257.

MITRA, A. & GREENBERG, M. D. 1984 Slow interactions of gravity waves and a corrugated sea bed. *Trans. ASME* E: *J. Appl. Mech.* **51**, 251–255.

PAPLINSKA, B. E., RUGELAND, T. & WERNER, G. 1983 Propagation of shallow-water waves in a hydraulic flume. *Bull. No.* 118. Hydraulics Laboratory, Royal Institute of Technology, Stockholm, Sweden.

PEREGRINE, D. H. 1972 Equations for water waves and the approximation behind them. In *Waves on Beaches* (ed. R. E. Meyer), pp. 95–121. Academic.

ROGERS, S. R. & MEI, C. C. 1978 Nonlinear resonant excitation of a long and narrow bay. *J. Fluid Mech.* **88**, 161–180.

SARPKAYA, T. & ISAACSON, M. 1981 *Mechanics of Wave Forces on Offshore Structures*, pp. 181–190. Van Nostrand Reinhold.

VENGAYIL, P. 1986 Shoaling and reflection of nonlinear shallow water waves. MS thesis, Department of Coastal and Oceanographic Engineering, University of Florida.